Costunolide attenuates oxygen-glucose deprivation/reperfusion-induced mitochondrial-mediated apoptosis in PC12 cells

LANQING MENG[1*], HUIXIA MA[1*], JINNI MENG[1*], TINGTING LI[2], YAFEI ZHU[2,3] and QIPENG ZHAO[1,2]

[1]Department of Pharmacology, School of Pharmacy, Ningxia Medical University; [2]Key Laboratory of Hui Ethnic Medicine Modernization, Ministry of Education, Ningxia Medical University; [3]College of Basic Medicine, Ningxia Medical University, Yinchuan, Ningxia Hui Autonomous Region 750004, P.R. China

Received November 22, 2020; Accepted March 4, 2021

DOI: 10.3892/mmr.2021.12050

Abstract. The present study investigated the effect of costunolide (CT), a compound extracted from *Aucklandia lappa* Decne, to attenuate oxygen-glucose deprivation/reperfusion (OGD/R)-induced mitochondrial-mediated apoptosis in PC12 cells. The present study used molecular docking technology to detect the binding of CT with mitochondrial apoptotic protein targets. A model of oxygen-glucose deprivation for 2 h and reperfusion for 24 h in PC12 cells was used to mimic cerebral ischemic injury. Cell viability and damage were measured using the Cell Counting kit-8 and lactate dehydrogenase (LDH) cytotoxicity assay kits. Cellular apoptosis was analyzed using flow cytometry. A fluorescence microscope determined intracellular [Ca^{2+}] and mitochondrial membrane potential. Furthermore, immunofluorescence and Western blot analyses were used to detect the expression of apoptosis-associated proteins. CT contains binding sites with Caspase-3, Caspase-9 and Caspase-7. CT markedly enhanced cell viability, inhibited LDH leakage, increased intracellular [Ca^{2+}], stabilized the mitochondrial membrane potential, increased the expression of Bcl-2 and inhibited the expression of Apaf-1, Bax, cleaved-caspase-7, cleaved-caspase-9 and cleaved-caspase-3. CT may markedly protect PC12 cells from damage caused by OGD/R, and its mechanism is associated with blocking the calcium channel and inhibiting mitochondrial-mediated apoptosis.

Correspondence to: Professor Qipeng Zhao, Key Laboratory of Hui Ethnic Medicine Modernization, Ministry of Education, Ningxia Medical University, 1160 Shengli Street, Xingqing, Yinchuan, Ningxia Hui Autonomous Region 750004, P.R. China
E-mail: zhqp623@126.com

Dr Yafei Zhu, College of Basic Medicine, Ningxia Medical University, 1160 Shengli Street, Xingqing, Yinchuan, Ningxia Hui Autonomous Region 750004, P.R. China
E-mail: 867453132@qq.com

*Contributed equally

Key words: costunolide, ischemic stroke, oxygen-glucose deprivation/reperfusion, apoptosis, caspase, PC12 cells

Introduction

Ischemic stroke is one of the most important causes of death and disability worldwide (1,2). In China, stroke became the top leading cause of mortality in 2017. Approximately 1.5 million people die from strokes each year (3). In ischemic stroke, the insufficient supply of oxygen and glucose causes brain damage within the subsequent few hours (4,5). The primary method is to restore the blood supply of ischemic brain tissue as soon as possible. However, the reopening of the occluded cerebrovascular usually leads to pathological damage in the ischemic tissue, which may further aggravate or potentially make the damage irreversible. Neuronal injury caused by ischemia/reperfusion is a complex process involving various mechanisms, including apoptosis, oxygen-free radicals, glutamic acid toxicity and [Ca^{2+}] overload (6). It remains an area of interest to perform drug research on stroke treatment (7).

Apoptosis is an essential mechanism of ischemic stroke (8,9). Apoptosis is regulated through the death receptor pathway, mitochondrial pathway and endoplasmic reticulum pathway. In the majority of vertebrates, apoptosis is regulated by the mitochondrial pathway (10,11). Mitochondria are the active centers of apoptosis regulation and the executors (12). The pro-apoptotic factor causes the mitochondrial permeability transition pore (MPTP) to open excessively, decreasing the membrane potential, releasing cytochrome c from the mitochondria to the cytosol. Next, caspase is activated and cells undergo apoptosis (13,14).

Mu-Xiang-You prescription is a classic prescription of Hui medicine, which affects ischemic stroke (15). *Aucklandia lappa* Decne is the main drug in the prescription (45% by weight); therefore, we hypothesized that *Aucklandia lappa* Decne is an essential drug in treating ischemic stroke. CT ($C_{15}H_{20}O_2$; Fig. 1), an active sesquiterpene lactone, is one of the main useful components of *Aucklandia lappa* Decne. CT is used to control the quality of *Aucklandia lappa* Decne in Chinese Pharmacopoeia. We hypothesized that the effect

of this prescription in the treatment of ischemic stroke is associated with CT. CT has multiple pharmacological activities, including inhibiting tumour cell proliferation (16) and decreasing the inflammatory response (17,18). However, it is unclear whether CT may attenuate cerebral ischemia/reperfusion injury and its anti-apoptosis mechanism. Therefore, the present study aimed to investigate the effects of CT and mechanisms on OGD/R-induced PC12 cell injury.

Materials and methods

Drugs and reagents. CT (cat. no. 447-43-0) was provided by the PUSH Bio-Technology. Fetal bovine serum and Dulbecco's modified Eagle's medium (DMEM) were offered by Gibco (Thermo Fisher Scientific, Inc.). Streptomycin and penicillin were purchased from HyClone (GE Healthcare Life Sciences). Nimodipine injection (cat. no. 12301323) was provided by Bayer Schering Pharma AG. Lactate dehydrogenase (LDH) assay kit (cat. no. 20090723), total protein extraction (cat. no. 20150323) and BCA protein quantification kits (kit no. 20150323) were provided by Nanjing Jiancheng Bioengineering Institute. ZSGB-BIO supplied horseradish peroxidase-conjugated goat anti-rabbit IgG secondary antibody (cat. no. ZB-2301). Primary antibodies against α-tubulin (cat. no. 2148), Apaf-1 (cat. no. 8723), Bcl-2 (cat. no. 2876) and Bax (cat. no. 2772) were provided by Cell Signaling Technology, Inc. Antibodies against procaspase-9 (cat. no. ab2013), procaspase-7 (cat. no. ab25900), cleaved-caspase-3 (cat. no. ab32042) and procaspase-3 (cat. no. ab44976) were provided by Abcam. Cleaved-caspase-7 (cat. no. AF4203), cleaved-caspase-9 (cat. no. AF5240) were supplied by Affinity Biosciences.

Molecular docking. The mol2, a molecular structure recording format designed by Sybyl molecular simulation software (version no. 2.1.1; Certara), the mol2 format of CT was downloaded from PubChem (http://pubchem.ncbi.nlm.nih.gov). CT and its interacting protein crystals (the structure is a protein complex with an inhibitor) were introduced into the Maestro 11.1 software ligprep module (Schrödinger, Inc.). The energy optimization of CT in the first field (OPLS-2005) was minimized. The structures of caspase-9, caspase-3 and caspase-7 with endogenous ligands were obtained from the Protein Data Bank. Using the Maestro 11.1 software Glide module, the target protein is modified, dehydrated and hydrogenated under default parameters. The active site of docking is generated by centering on the original ligand. Finally, CT is molecularly docked with the target protein (Fig. 2).

Cell culture. The PC12 cells were obtained from the rat adrenal medulla of pheochromocytoma and have been widely used as an *in vitro* cellular model of neurological diseases and cell signal transduction pathways due to its sympathetic neuron's physiological characteristics. PC12 cells were provided by the Chinese Academy of Sciences Shanghai Cell Biology Institute. PC12 cells were cultured in high-glucose DMEM supplemented with 5% fetal calf serum, streptomycin (100 μg/ml), penicillin (100 U/ml) and 5% CO_2 at 37˚C (19,20).

Drug treatment. A stock solution was prepared using dimethyl sulfoxide, CT concentrations were set at 2.5, 5 and 10 μM according to our preliminary experimental results. Nimodipine is a calcium channel blocker, and it was used as a positive control drug in this experiment at a concentration of 5 μM (21). Prior to the investigation, the cells were inoculated in culture plates at a density of $1.0x10^5$ cells/ml. After 12 h of adhering, to initiate oxygen-glucose deprivation (OGD) by replacing the cell culture medium with the glucose-free medium, the cells were incubated for 2 h in an oxygen-free chamber (5% CO_2; 95% N_2) at 37˚C. At the end of the OGD period, the cells were incubated under normal growth conditions (5% CO_2 and 95% O_2) for 24 h to achieve reperfusion (R) (22). Cells in the experimental groups were treated with CT (2.5, 5 or 10 μM) and Nimodipine (5 μM) during the entire period of OGD/R.

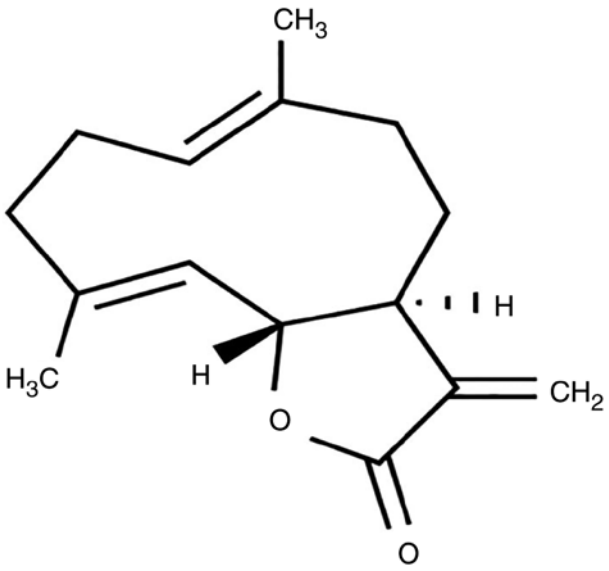

Figure 1. Chemical structure of CT. The molecular formula for CT is C_{15} H_{20} O_2 and the molecular weight is 232.32 kD. CT, costunolide.

Morphological changes in cells. Following OGD/R, the cells were washed three times with PBS, and the inverted microscope (Olympus Corporation; TH4-200; magnification, x200) was used to capture the images.

CCK-8 assay and LDH release assay. A CCK-8 assay measured the cell viability, according to the manufacturer's protocols. PC12 cells were cultured in 96-well plates ($1x10^4$ cells/well) and, following OGD/R, CCK-8 (10 μl per well) was added, and cells were incubated for 4 h at 37˚C. The OD value at the wavelength of 450 nm was detected by an enzyme labeling instrument.

Cytotoxicity was assessed by measuring the level of LDH in the culture medium. Following reperfusion, the medium was collected for LDH level measurement. The LDH level was measured by spectrophotometry determination at 440 nm, according to the manufacturer's protocol. The release of LDH reflects the degree of cell damage.

Flow cytometric apoptosis assay. The percentage of the apoptotic cells was determined using an Annexin V-FITC/PI kit (Nanjing KeyGen Biotech Co., Ltd.). The PC12 cells were cultured in 6-well plates ($1x10^6$ cells/well), washed twice with ice-cold PBS following treatment, collected by trypsinization

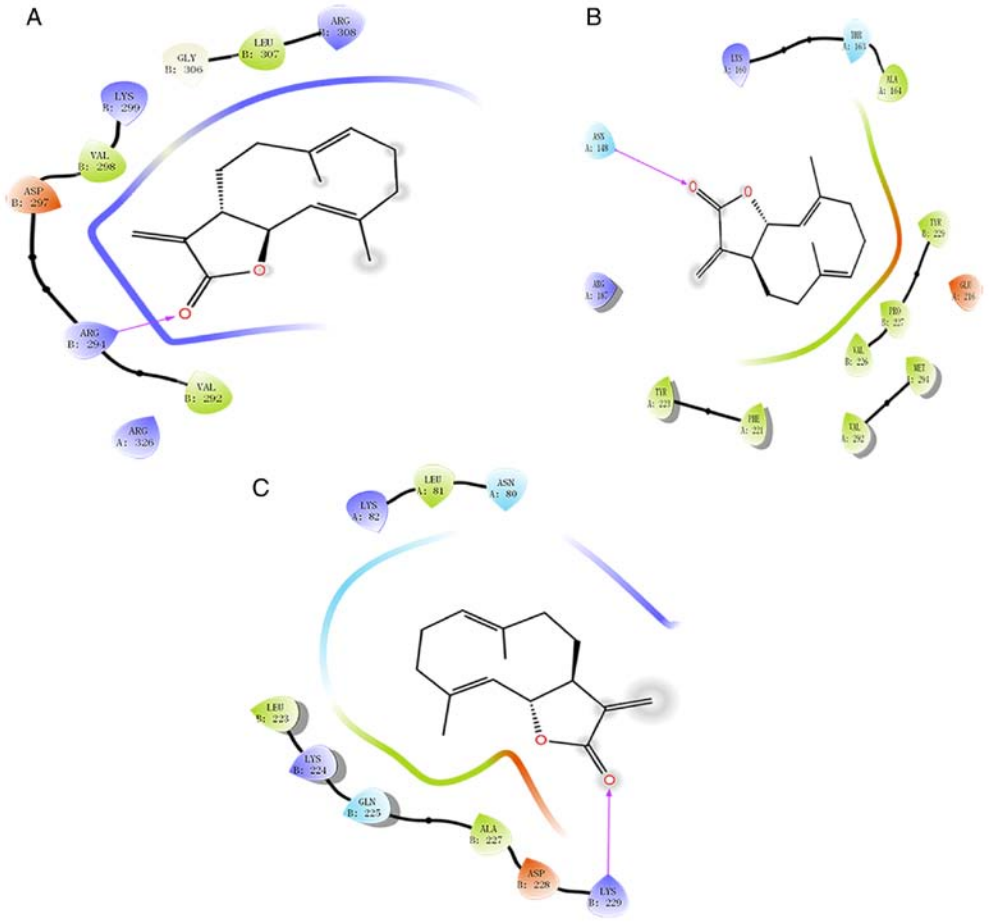

Figure 2. Molecular binding mode in the protein domains of CT docking. (A) Caspase-9, (B) Caspase-7 and (C) Caspase-3. Droplet shapes represent amino acid groups that interact with CT in 4Å. Capital letters represent the abbreviation for amino acids. The numbers represent the numbering of amino acids in proteins. The line represents the CT in the protein cavity. The arrow mark indicates hydrogen bonding interactions between CT and protein domain residues. CT, costunolide.

without EDTA. Next, cells were suspended in 400 μl 1X Annexin V and then Annexin V-FITC staining fluid 5 μl was added in the dark, at 4˚C for 15 min, prior to 10 μl PI staining fluid being added at 4˚C for 5 min. Finally, the cells were analyzed by flow cytometry (BD Biosciences) using BD Accuri C6 software (version no. 1.0.264.21; BD Biosciences) The total apoptosis rate is equal to the early apoptotic rate plus the dead cells rate.

Mitochondrial membrane potential (MMP) measurement. Disruption of the MMP is one of the earliest intracellular changes following apoptosis induction (19). It has been reported that the decrease in MMP is associated with the apoptosis of numerous types of cells (23). JC-1 is a probe commonly used to detect the MMP of cells. When the MMP is high, JC-1 may accumulate in the mitochondrial matrix and form polymers to generate red fluorescence. When the MMP is low, the monomer state glows green. Following reperfusion, the cells were washed twice with PBS. Next, the cells were pretreated and stained according to the method of the MMP detection kit (Nanjing KeyGen Biotech Co., Ltd.). The fluorescence microscope (IX-73; Olympus Corporation; magnification, x200) detected the intensity of fluorescence in each group.

Intracellular [Ca^{2+}] measurement. Fluo-3 AM is the most commonly used for the detection of intracellular [Ca^{2+}]. Following reperfusion, the PC12 cells were washed twice with PBS and incubated with 5 μM/l Fluo-3/AM staining solution at 37˚C for 30 min in the dark. Subsequently, the cells were washed twice with PBS. Next, with a fluorescence microscope (IX-73; Olympus Corporation; magnification, x200) to observe the fluorescence intensity.

Western blot analysis. The protein expression of Apaf-1, cleaved-caspase-7, procaspase-7, cleaved-caspase-3, procaspase-3, cleaved-caspase-9, procaspase-9, Bcl-2 and Bax in the cells following OGD/R injury were detected by Western blotting. Following treatment, cells were collected and cell lysates were prepared by incubation in RIPA buffer containing a protease inhibitor cocktail (Beijing Leagene Biotech Co., Ltd.) according to the manufacturer's protocols. Following protein concentration estimation using a BCA protein quantitation assay kit (Nanjing KeyGen Biotech Co., Ltd.), equal amounts (30 μg) of proteins were separated via 10% SDS-PAGE, prior to being transferred to a PVDF membrane. The membranes were blocked with 5% skimmed dry milk in tris-buffer solution (TBST) for 2 h at room temperature. Membranes were incubated with primary antibodies for overnight at 4˚C, and the primary antibodies used were as follows: Bcl-2 (dilution, 1:1,000), Bax (dilution, 1:300), Apaf-1 (dilution, 1:300), procaspase-9 (dilution, 1:1,000), procaspase-7 (dilution, 1:500),

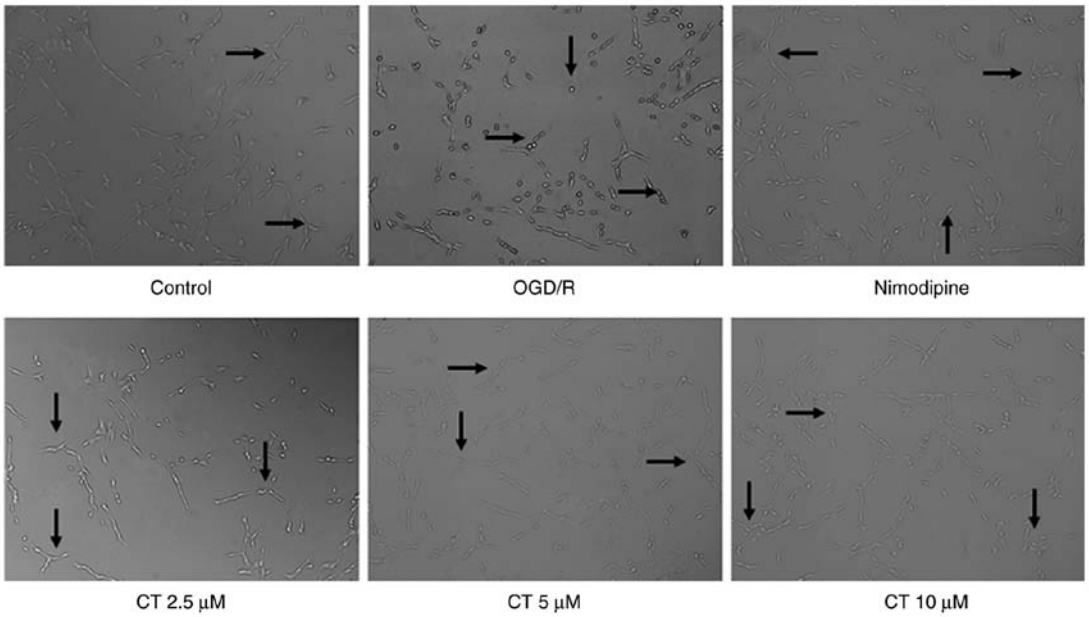

Figure 3. Effect of CT on the morphology of the OGD/R injury model in PC12 cells (magnification, x200). The arrow points to the cells with morphological changes. CT, costunolide; OGD/R, oxygen-glucose deprivation/reperfusion.

procaspase-3 (dilution, 1:500), cleaved-caspase-3 (dilution, 1:500), cleaved-caspase-7 (dilution, 1:500), cleaved-caspase-9 (dilution, 1:500) and α-tubulin (dilution, 1:1,000). Next, labelled membranes were washed with TBST three times, and the membrane was probed with an HRP-labeled secondary antibody (dilution, 1:2,000; BIOSS) for 1 h at room temperature. The bands were then visualized using the Amersham Imager 600 imaging system (GE Healthcare Life Sciences).

Immunofluorescence detection. Immunofluorescence was detected to investigate the expression of Bcl-2 and Bax. Following reperfusion, the cells were washed 3 times with PBS, then post-fixed in 4% paraformaldehyde at room temperature for 20 min and incubated in 0.3% Triton X-100 for a further 20 min. Cells were washed with PBS and blocked with 1% BSA at 37˚C for 2 h. Next, Bcl-2 (dilution, 1:100) and Bax (dilution, 1:100) antibodies were added and incubated overnight. Cells were washed with PBS, fluorescent second antibody (dilution, 1:500) was added and incubated for 2 h in the dark at room temperature, the cells were washed 3 times with PBS, and DAPI (dilution, 1:500) was added for 30 min. Finally, cells were viewed using a fluorescence microscope (Olympus IX71; Olympus Corporation; magnification, x100).

Statistical analysis. The data were analyzed by Image Proplus and SPSS 17.0 software (SPSS, Inc.). Data are presented as the mean ± standard deviation, and the changes in variable parameters were analyzed by one-way analysis of variance, followed by the Dunnett's test. $P<0.05$ was considered to indicate a statistically significant difference.

Results

Results of molecular docking. Molecular docking was used to predict the probable targets of CT. The docking results revealed a high affinity of CT towards Caspase-9, Caspase-3 and Caspase-7 (Fig. 2). Caspase-9 showed interactions between CT and Gly306, Leu307, Arg308, Val292, Arg294, Asp297, Val298 and Lys299 forming a hydrogen bond effect. Specifically, CT and an active site with residues Arg294 forms a hydrogen bond effect. Caspase-7 was interacting with CT through Val226, Pro227, Tyr229, Lys160, Thr163, Ala164, Tyr223 and Phe221. Specifically, CT and an active site with residues, Asn148, forms a hydrogen bond effect. CT was interacting with the Lys82, Leu81, Asn80, Lbu223, Lys224, Gln225, Ala227 and Asp228 residues of Caspase-3 form a strong hydrophobic effect. Specifically, CT and an active site with residues, Lys229, form a hydrogen bond effect.

Effect of CT on PC12 cell morphological changes. The results demonstrated that the number of PC12 cells significantly decreased following OGD/R treatment, certain cells became round or floating, and the cells exhibited typical swelling. Compared with the OGD/R group, in the OGD/R+CT group (2.5, 5 and 10 μM), the cell body was relatively full, the membrane was smooth and intact, and the adhesion was good (Fig. 3). The results indicated that CT has a protective effect on PC12 cell injury induced by OGD/R.

Effect of CT on PC12 cell viability and cell cytotoxicity. As shown in Fig. 4A, PC12 cell viability was significantly decreased following the cell being exposed to OGD for 2 h and reperfusion for 24 h. Following treatment with CT (2.5 and 5 μM), PC12 cell viability was significantly increased ($P<0.05$). LDH assays were performed as shown in Fig. 4B, and it was revealed that CT (2.5, 5 and 10 μM) significantly attenuated OGD/R-induced LDH leakage.

Effects of CT on apoptosis in PC12 cells. FITC-Annexin V/PI double staining was used with flow cytometry to analyze the anti-apoptotic capacity of CT under OGD/R conditions (Fig. 5). The results demonstrated that the cell apoptotic rate

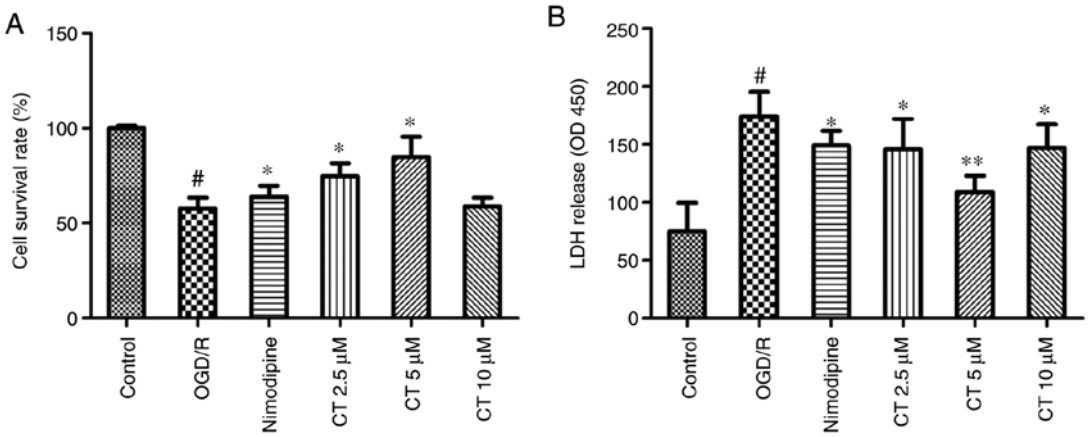

Figure 4. Effects of CT on (A) cell survival and (B) LDH release in PC12 cells following OGD/R. Values are presented as the mean ± standard deviation (n=10). #P<0.05, compared with the control group; *P<0.05 and **P<0.01, compared with the OGD/R group. CT, costunolide; OGD/R, oxygen-glucose deprivation/reperfusion; OD, optical density; LDH, lactate dehydrogenase.

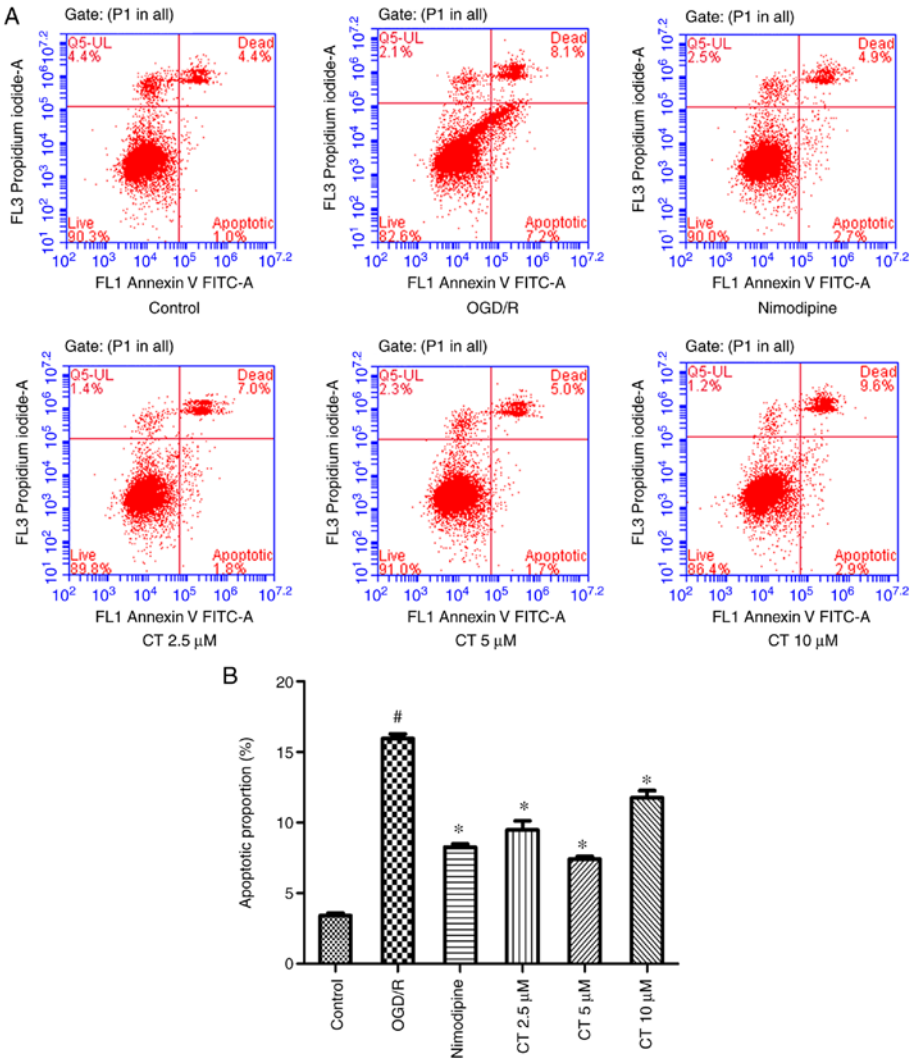

Figure 5. Effect of CT on the apoptotic rate following OGD/R in PC12 cells. (A) Cell apoptosis was determined by flow cytometry. (B) Quantitative analysis of apoptotic rate. Values are presented as the mean ± standard deviation (n=3). #P<0.05, compared with control group; *P<0.05, compared with the OGD/R group. CT, costunolide; OGD/R, oxygen-glucose deprivation/reperfusion.

was significantly decreased following treatment with CT (2.5, 5 and 10 μM). The apoptotic cell rate with CT (10 μM) was higher than CT (5 μM), consistent with the effect of CT on the PC12 cell viability assay following OGD/R injury.

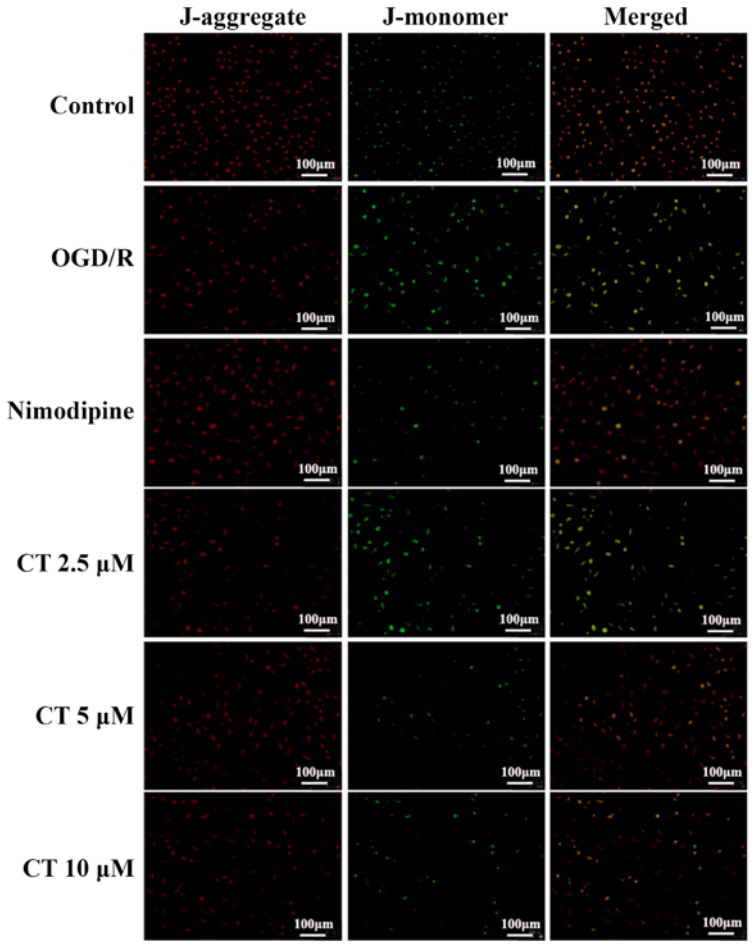

Figure 6. Effect of CT on mitochondrial membrane potential in PC12 cells following OGD/R injury (magnification, x200). The left image shows the JC-1 aggregate form, the middle image shows the JC-1 monomer form, and the right image shows the merge of the left and central images. CT, costunolide; OGD/R, oxygen-glucose deprivation/reperfusion.

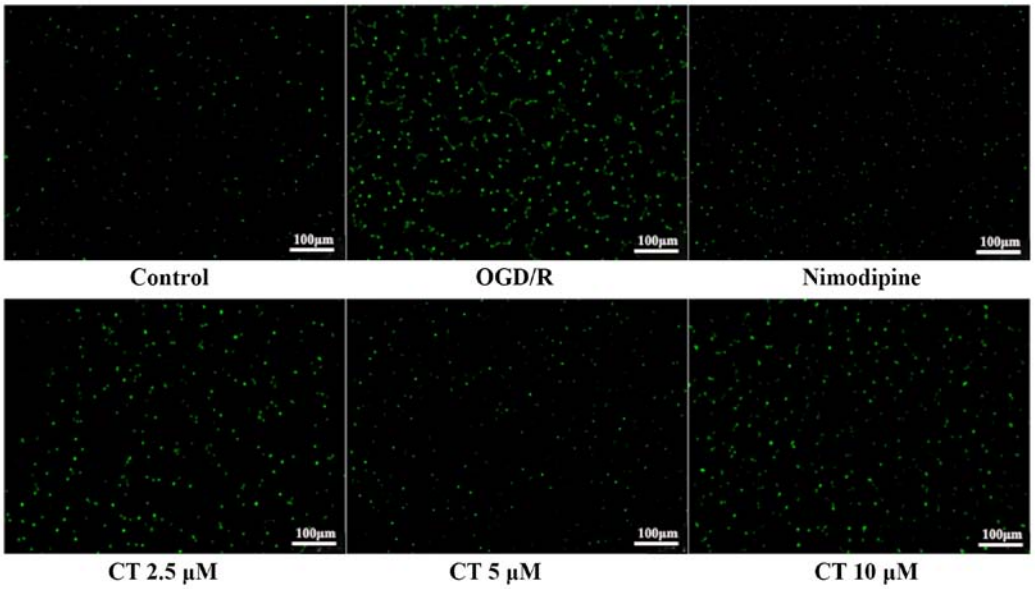

Figure 7. Effects of CT on intracellular [Ca^{2+}] concentration in PC12 cells following OGD/R injury (magnification, x200). The CT (2.5, 5 and 10 μM) decreased the intracellular [Ca^{2+}] concentration. CT, costunolide; OGD/R, oxygen-glucose deprivation/reperfusion.

Effects of CT on MMP in PC12 cells. Fluorescence microscopy was used to detect MMP. Following treatment with the CT (2.5, 5 and 10 μM), red fluorescence increased in varying degrees, respectively, compared with the OGD/R group (Fig. 6).

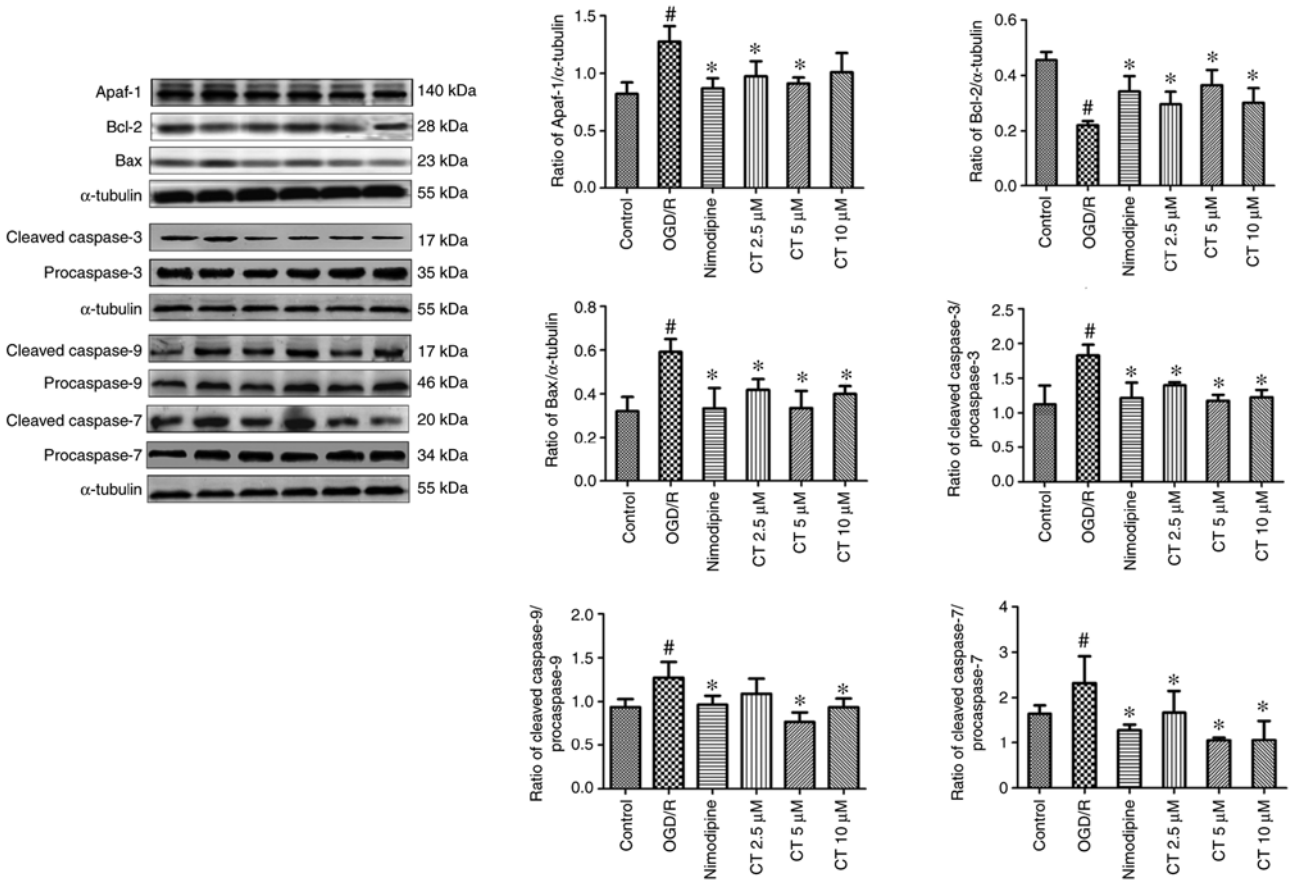

Figure 8. Effects of CT on the expression of Apaf-1, Bcl-2, Bax, cleaved-Caspase-9, cleaved-Caspase-7, cleaved-Caspase-3 in PC12 cells following OGD/R. The stripe diagram represents Western blot analysis of Apaf-1, Bcl-2, Bax, cleaved-Caspase-9, cleaved-Caspase-7, cleaved-Caspase-3, procaspase-9, procaspase-7 and procaspase-3. α-tubulin was usedd as the loading control. The bar chart represents the quantitative analysis of Apaf-1, Bcl-2, Bax, cleaved-Caspase-9/procaspase-9, cleaved-Caspase-7/procaspase-7 and cleaved-Caspase-3/procaspase-3 expression. Values are presented as the mean ± standard deviation (n=3). #P<0.05, compared with the control group; *P<0.05, compared with OGD/R group. CT, costunolide; OGD/R, oxygen-glucose deprivation/reperfusion.

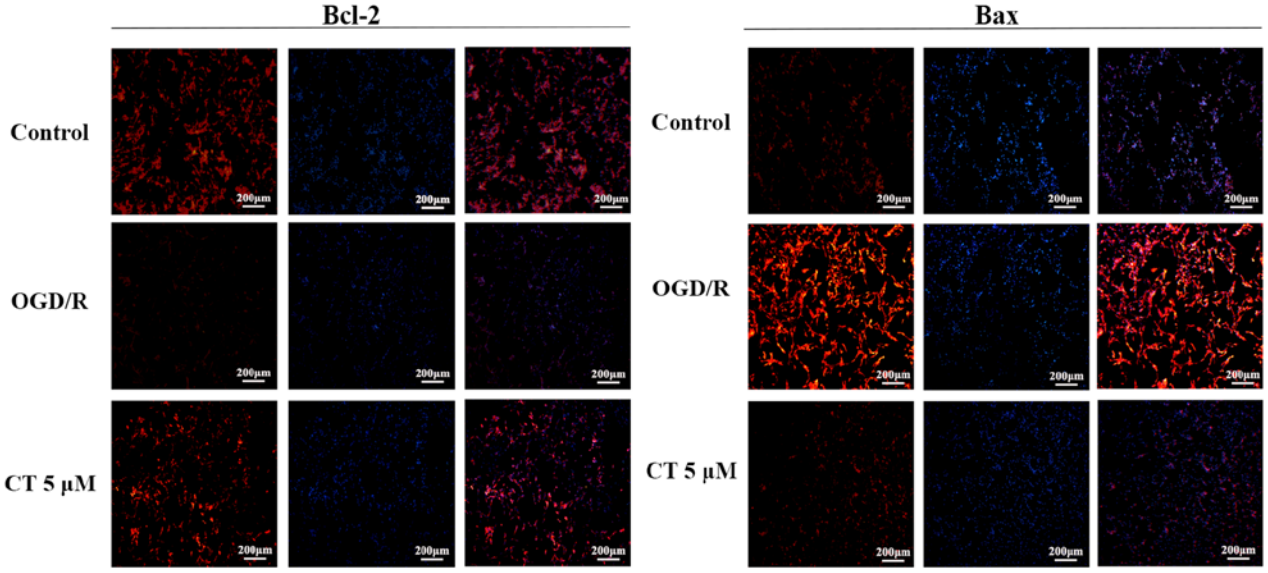

Figure 9. Effects of CT on the expression of Bcl-2 and Bax in PC12 cells following OGD/R (magnification, x100). The left image shows immunofluorescent staining with specific markers. The middle image shows the staining of the nucleus with DAPI. The right image shows the merge of the left and middle images. CT, costunolide; OGD/R, oxygen-glucose deprivation/reperfusion.

Effects of CT on intracellular [Ca^{2+}] in PC12 cells. As a second messenger, [Ca^{2+}] regulates signal transduction and neurotransmitter release (24,25). Compared with the control group, the green fluorescence of the OGD/R group was very

strong, which indicated that OGD/R increased the [Ca^{2+}] concentration in PC12 cells. The green fluorescence of cells treated with CT (2.5, 5 and 10 μM) was decreased, suggesting that CT decreased intracellular [Ca^{2+}] concentration. The results demonstrated that CT could inhibit the increase of intracellular [Ca^{2+}] induced by OGD/R injury (Fig. 7).

Effects of CT on the expression of Apaf-1, cleaved-Caspase-3, Caspase-3,cleaved-Caspase-7,Caspase-7,cleaved-Caspase-9, Caspase-9, Bax and Bcl-2 in PC12 cells following OGD/R. The expression of Bax and Apaf-1 were significantly increased following OGD/R. CT (2.5, 5 and 10 μM) inhibited the expression of Bax and Apaf-1. Additionally, following treatment of PC12 cells with OGD/R, the expression of Bcl-2 was decreased, treatment with CT (2.5, 5 and 10 μM) significantly attenuated the decrease in the Bcl-2 expression (Fig. 8).

In the present study, the expression of cleaved-Caspase-3, cleaved-Caspase-7, cleaved-Caspase-9, procaspase-3, procaspase-7 and procaspase-9 was investigated. As shown in Fig. 8, compared with the control group, the expression of cleaved-Caspase-9, cleaved-Caspase-3 and cleaved-Caspase-7 were significantly enhanced following OGD/R. CT (2.5, 5 and 10 μM) may markedly inhibit the expression of these proteins.

Detection of Bcl-2 and Bax in PC12 cells following OGD/R by cellular immunofluorescence. The expression of Bcl-2 protein was significantly decreased following OGD/R. However, following the intervention with CT (5 μM), red fluorescence was enhanced, which indicated that CT may improve the expression of Bcl-2 (Fig. 9). As shown in Fig. 9, the expression of Bax was notably increased following OGD/R compared with the control group. Compared with the OGD/R group, red fluorescence became weaker, which indicated that CT may inhibit the expression of Bax.

Discussion

Molecular docking is a drug design method that follows the characteristics of the receptor, and the interaction between the receptor and the drug molecule (26). Proteins may undergo conformational transitions in physiological environments, and these transitions may stabilize following ligand binding (27). Drugs are small compounds that act by binding to or interacting with a protein kinase. The intermolecular interactions between protein and medicines may be due to hydrophobic interactions, electrostatic and van der Waals forces (28). The results demonstrated that CT contains binding sites with Caspase-9, Caspase-7 and Caspase-3. It suggested that these proteins may be the target of CT anti-apoptosis.

According to a previous study, the PC12 injury model induced by OGD/R is often used to mimic cerebral ischemia/reperfusion injury (29). This model was used in the present study to investigate the effect and mechanisms of CT. The results demonstrated that CT may protect PC12 cells from OGD/R-induce injury by enhancing cell viability and inhibiting LDH leakage.

Apoptosis plays an essential role in maintaining metabolic balance and controlling neuron damage. Available evidence has suggested that apoptosis serves a significant role in the cerebral ischemia/reperfusion process (30,31). The results of the present study demonstrated that the number of apoptotic cells increased significantly following OGD/R. CT (2.5, 5 and 10 μM) significantly decreased apoptosis cells. However, the anti-apoptotic effect of 10 μM CT was not as significant as that of 5 μM CT. In early experiments on the cytotoxicity of CT on PC12 cells, it was found that after the CT dose increased to 10 μM, it became cytotoxic, which led to an increase in apoptosis. Therefore, it may cause the apoptotic cell rate with 10 μM CT to be higher than 5 μM CT, but the toxicity of 10 μM CT is minimal, and it has a specific protective effect on PC12 cells following OGD/R injury. Therefore, 5 μM CT has a better anti-apoptotic effect than 10 μM CT. MMP is a sensitive indicator reflecting mitochondrial function. The decrease in MMP leads to instability of neuronal cell structure, thereby causing cell damage and ultimately results in cell death (22). A recent study has confirmed that OGD/R may cause intracellular [Ca^{2+}] overload and lead to mitochondrial dysfunction, resulting in unstable neuronal cell structure and ultimately leading to neuronal apoptosis (32). Following treatment with OGD/R in PC12 cells, the MMP decreased, and the intracellular [Ca^{2+}] increased. However, CT decreased intracellular [Ca^{2+}] overload and enhanced MMP. These results indicated that CT has a protective role in PC12 cell injury induced by OGD/R.

A mitochondria-mediated apoptosis signalling pathway is one of the main pathways in the apoptotic of cerebral ischemia-reperfusion injury. The Bcl-2 protein family and its members form an incredibly complex network of interactions that regulate apoptosis. These proteins serve an essential role in regulating and controlling apoptosis (33). Bcl-2 is an essential anti-apoptotic protein that may stabilize mitochondrial membrane function and prevent mitochondria release Cyto-c (34). Bax is a pro-apoptotic protein in the cytoplasm under normal conditions. Bax increases the permeability of the mitochondrial membrane, which leads to the release of Cyto-c under certain stimulating conditions (35,36). Next, in the presence of dATP, Cyto-c binds to Apaf-1 to catalyze the activation of Caspase-9, and then activate downstream effector Caspases, including Caspase-3, Caspase-6 and Caspase-7, which in turn execute apoptosis by cleaving cellular proteins following specific Asp residues (37). In the mitochondria-mediated pathway, Caspase-3 is the main influencing factor in the process of apoptosis, and its activation is a sign that the cell is entering an irreversible stage of apoptosis (15). In the present study, the expression levels of Bcl-2 decreased, while the protein levels of Bax, Apaf-1, cleaved-Caspase-9, cleaved-Caspase-3 and cleaved-Caspase-7 significantly increased in OGD/R-treated PC12 cells. These results were consistent with those reported in the literature (38,39). Reversal of these CT trends suggested that the protective effect of CT may be associated with the inhibition of mitochondrial-mediated apoptosis in PC12 cells.

Costunolide had a protective effect against OGD/R-induced PC12 cell injury, and the mechanism may be associated with the inhibition of mitochondrial-mediated apoptosis.

Acknowledgements

Not applicable.

Funding

The present study was supported by the National Natural Science Foundation of Ningxia (grant no. 2020AAC02017) and the National Natural Science Foundation of China (grant no. 81660700).

Availability of data and materials

The datasets used and/or analyzed during the current study are available from the corresponding author on reasonable request.

Authors' contributions

LM, HM and JM established the PC12 cell injury model induced by OGD/R, and were responsible for detecting cell viability, LDH, [Ca^{2+}] concentration, mitochondrial membrane potential and protein expression. TL and HM analyzed and interpreted the data. LM wrote the manuscript. YZ and QZ designed the study, supervised the research group and revised the manuscript critically for important intellectual content. YZ and QZ confirmed the authenticity of all the raw data. The final version of the manuscript was read and approved by all authors.

Ethics approval and consent to participate

Not applicable.

Patient consent for publication

Not applicable.

Competing interests

The authors declare that they have no competing interests.

References

1. Katan M and Luft A: Global burden of stroke. Semin Neurol 38: 208-211, 2018.
2. Nitzsche A, Poittevin M, Benarab A, Philippe Bonnin P, Faraco G, Uchida H, Favre J, Garcia-Bonilla L, Garcia MCL, Léger PL, *et al*: Endothelial S1P signaling counteracts infarct expansion in ischemic stroke. Circ Res 128: 363-382, 2021.
3. Tu WJ, Zeng XW, Deng A, Zhao SJ, Luo DZ, Ma GZ, Wang H and Liu Q: Circulating FABP4 (Fatty Acid-Binding Protein 4) is a novel prognostic biomarker in patients with acute ischemic stroke. Stroke 48: 1531-1538, 2017.
4. Brassai A, Suvanjeiev RG, Bán EG and Lakatos M: Role of synaptic and nonsynaptic glutamate receptors in ischaemia induced neurotoxicity. Brain Res Bull 112: 1-6, 2015.
5. Maier O, Menze BH, Von der Gablentz J, Häni L, Heinrich MP, Liebrand M, Winzeck S, Basit A, Bentley P, Chen L, *et al*: ISLES 2015-A public evaluation benchmark for ischemic stroke lesion segmentation from multispectral MRI. Med Image Anal 35: 250-269, 2017.
6. Zhao J, Bai Y, Zhang C, Zhang X, Zhang YX, Chen J, Xiong L, Shi M and Zhao G: Cinepazide maleate protects PC12 cells against oxygen-glucose deprivation-induced injury. Neurol Sci 35: 875-881, 2014.
7. Zhao QP, Chen AL, Wang XB, Zhang ZH, Zhao YH, Huang Y, Ren SG and Zhu Y: Protective effects of dehydrocostuslactone on rat hippocampal slice injury induced by oxygen-glucose deprivation/reoxygenation. Int J Mol Med 42: 1190-1198, 2018.
8. Li ZR, Yang L, Zhen J, Zhao Y and Lu ZN: Nobiletin protects PC12 cells from ERS-induced apoptosis in OGD/R injury via activation of the PI3K/AKT pathway. Exp Ther Med 16: 1470-1476, 2018.
9. Meng X, Xie W, Xu Q, Liang T, Xu X, Sun G and Sun X: Neuroprotective effects of radix scrophulariae on cerebral ischemia and reperfusion injury via MAPK pathways. Molecules 23: 2401, 2018.
10. Kerr JF and Searle J: A suggested explanation for the paradoxically slow growth rate of basal-cell carcinomas that contain numerous mitotic figures. J Pathol 107: 41-44, 1972.
11. Green DR and Kroemer G: The pathophysiology of mitochondrial cell death. Science 305: 626-629, 2004.
12. Zamzami N, Hirsch T, Dallaporta B, Petit PX and Kroemer G: Mitochondrial implication in accidental and programmed cell death: Apoptosis and necrosis. J Bioenerg Biomembr 29: 185-193, 1997.
13. Song XF, Tian H, Zhang P and Zhang ZX: Expression of Cyt-c-mediated mitochondrial apoptosis-related proteins in rat renal proximal tubules during development. Nephron 135: 77-86, 2017.
14. Malladi S, Challa-Malladi M, Fearnhead HO and Bratton SB: The Apaf-1*procaspase-9 apoptosome complex functions as a proteolytic-based molecular timer. EMBO J 28: 1916-1925, 2009.
15. Zhao Q, Cheng X, Wang X, Wang J, Zhu Y and Ma X: Neuroprotective effect and mechanism of Mu-Xiang-You-Fang on cerebral ischemia-reperfusion injury in rats. J Ethnopharmacol 192: 140-147, 2016.
16. Cai H, He X and Yang C: Costunolide promotes imatinib-induced apoptosis in chronic myeloid leukemia cells via the Bcr/Abl-Stat5 pathway. Phytother Res 32: 1764-1769, 2018.
17. Chen Z, Zhang D, Li M and Wang B: Costunolide ameliorates lipoteichoic acid-induced acute lung injury via attenuating MAPK signaling pathway. Int Immunopharmacol 61: 283-289, 2018.
18. Saraswati S, Alhaider AA and Abdelgadir AM: Costunolide suppresses inflammatory angiogenic response in a subcutaneous murine sponge model. APMIS 126: 257-266, 2018.
19. Zhang C, Li C, Chen S, Li Z, Jia X, Wang K, Bao J, Liang Y, Wang X, Chen M, *et al*: Berberine protects against 6-OHDA-induced neurotoxicity in PC12 cells and zebrafish through hormetic mechanisms involving PI3K/AKT/Bcl-2 and Nrf2/HO-1 pathways. Redox Biol 11: 1-11, 2017.
20. Zhang JF, Zhang L, Shi LL, Zhao ZH, Xu H, Liang F, Li HB, Zhao Y, Xu X, Yang K and Tian YF: Parthenolide attenuates cerebral ischemia/reperfusion injury via Akt/GSK-3βpathway in PC12 cells. Biomed Pharmacother 89: 1159-1165, 2017.
21. Wang H, Wei W, Lan XB, Liu N, Li Y, Ma H, Sun T, Peng X, Zhuang C and Yu J: Neuroprotective effect of swertiamain on cerebral ischemia/reperfusion injury by inducing the Nrf2 protective pathway. ACS Chem Neurosci 10: 2276-2286, 2019.
22. Ma HX, Hou F, Chen AL, Li TT, Zhu YF and Zhao QP: Mu-Xiang-You-Fang protects PC12 cells against OGD/R-induced autophagy via the AMPK/mTOR signaling pathway. J Ethnopharmacol 252: 112583, 2020.
23. Jangholi E, Sharifi ZN, Hoseinian M, Zarrindast MR, Rahimi HR, Mowla A, Aryan H, Javidi MA, Parsa Y, Ghaffarpasand F, *et al*: Verapamil inhibits mitochondria-induced reactive oxygen species and dependent apoptosis pathways in cerebral transient global ischemia/reperfusion. Oxid Med Cell Longev 2020: 5872645, 2020.
24. Farajdokht F, Mohaddes G, Karimi-Sales E, Kafshdooz T, Mahmoudi J, Aberoumandi SM and Karimi P: Inhibition of PTEN protects PC12 cells against oxygen-glucose deprivation induced cell death through mitoprotection. Brain Res 1692: 100-109, 2018.
25. Seta K, Kim HW, Ferguson T, Kim R, Pathrose P, Yuan Y, Lu G, Spicer Z and Millhorn DE: Genomic and physiological analysis of oxygen sensitivity and hypoxia tolerance in PC12 cells. Ann N Y Acad Sci 971: 379-388, 2002.
26. Kuntz ID, Blaney JM, Oatley SJ, Langridge R and Ferrin TE: A geometric approach to macromolecule-ligand interactions. J Mol Biol 161: 269-288, 1982.
27. Overington JP, Bissan AL and Hopkins AL: How many drug targets are there? Nat Rev Drug Discov 5: 993-996, 2006.
28. Naqvi AAT, Mohammad T, Hasan GM and Hassan MI: Advancements in docking and molecular dynamics simulations towards ligand-receptor interactions and structure-function relationships. Curr Top Med Chem 8: 1755-1768, 2018.
29. Feng LY, Gao JM, Liu YG, Shi JS and Gong Q: Icariside II alleviates oxygen-glucose deprivation and reoxygenation-induced PC12 cell oxidative injury by activating Nrf2/SIRT3 signaling pathway. Biomed Pharmacother 103: 9-17, 2018.

30. Broughton BR, Reutens DC and Sobey CG: Apoptotic mechanisms after cerebral ischemia. Stroke 40: e331-e339, 2009.
31. Zhu JR, Tao YF, Lou S and Wu ZM: Protective effects of ginsenoside Rb(3) on oxygen and glucose deprivation-induced ischemic injury in PC12 cells. Acta Pharmacol Sin 31: 273-280, 2010.
32. de Pablo Y, Nilsson M, Pekna M and Pekny M: Intermediate filaments are important for astrocyte response to oxidative stress induced by oxygen-glucose deprivation and reperfusion. Histochem Cell Biol 140: 81-91, 2013.
33. Zheng YQ, Liu JX, Li XZ, Xu L and Xu YG: RNA interference-mediated downregulation of Beclin1 attenuates cerebral ischemic injury in rats. Acta Pharmacol Sin 30: 919-927, 2009.
34. Adams KW and Cooper GM: Rapid turnover of mcl-1 couples translation to cell survival and apoptosis. J Biol Chem 282: 6192-6200, 2007.
35. Kim J, Parrish AB, Kurokawa M, Matsuura K, Freel CD, Andersen JL, Johnson CE and Kornbluth S: Rsk-mediated phosphorylation and 14-3-3βbinding of Apaf-1 suppresses cytochrome c-induced apoptosis. EMBO J 31: 1279-1292, 2012.
36. Liu X, Zhu X, Chen M, Ge Q, Shen Y and Pan S: Resveratrol protects PC12 cells against OGD/R-induced apoptosis via the mitochondrial-mediated signaling pathway. Acta Biochim Biophys Sin (Shanghai) 48: 342-353, 2016.
37. Boatright KM and Salvesen GS: Mechanisms of caspase activation. Curr Opin Cell Biol 15: 725-731, 2003.
38. Guo H, Chen L, Cui H, Peng X, Fang J, Zuo Z, Deng J, Wang X and Wu B: Research advances on pathways of nickel-induced apoptosis. Int J Mol Sci 17: 10-19, 2015.
39. Haddad JJ: The role of Bax/Bcl-2 and pro-caspase peptides in hypoxia/reperfusion-dependent regulation of MAPKERK: Discordant proteomic effect of MAPK(p38). Protein Pept Lett 14: 361-371, 2007.